ARTICLE

Causative Mutations and Mechanism of Androgenetic Hydatidiform Moles

Ngoc Minh Phuong Nguyen,[1,15] Zhao-Jia Ge,[1,15] Ramesh Reddy,[1] Somayyeh Fahiminiya,[1,2] Philippe Sauthier,[3] Rashmi Bagga,[4] Feride Iffet Sahin,[5] Sangeetha Mahadevan,[6] Matthew Osmond,[1,2] Magali Breguet,[3] Kurosh Rahimi,[7] Louise Lapensee,[8,9] Karine Hovanes,[10] Radhika Srinivasan,[11] Ignatia B. Van den Veyver,[6] Trilochan Sahoo,[10] Asangla Ao,[1,12] Jacek Majewski,[1,2] Teruko Taketo,[12,13,14] and Rima Slim[1,12,*]

Androgenetic complete hydatidiform moles are human pregnancies with no embryos and affect 1 in every 1,400 pregnancies. They have mostly androgenetic monospermic genomes with all the chromosomes originating from a haploid sperm and no maternal chromosomes. Androgenetic complete hydatidiform moles were described in 1977, but how they occur has remained an open question. We identified bi-allelic deleterious mutations in *MEI1*, *TOP6BL/C11orf80*, and *REC114*, with roles in meiotic double-strand breaks formation in women with recurrent androgenetic complete hydatidiform moles. We investigated the occurrence of androgenesis in *Mei1*-deficient female mice and discovered that 8% of their oocytes lose all their chromosomes by extruding them with the spindles into the first polar body. We demonstrate that $Mei1^{-/-}$ oocytes are capable of fertilization and 5% produce androgenetic zygotes. Thus, we uncover a meiotic abnormality in mammals and a mechanism for the genesis of androgenetic zygotes that is the extrusion of all maternal chromosomes and their spindles into the first polar body.

Introduction

Hydatidiform mole (HM) (MIM: 231090) is a human pregnancy with abnormal embryonic development and excessive trophoblastic proliferation. The common form of HM is sporadic, non-recurrent, and affects 1 in every 600 pregnancies.[1] Based on microscopic morphological evaluation, half of common HMs belong to the histological type of partial HMs (PHMs) and have a triploid dispermic genome with two sets of paternal chromosomes and one set of maternal chromosomes. The second half belongs to the histological type of complete HMs (CHMs) and has a diploid androgenetic genome with all the chromosomes originating from one (monospermic) or two sperms (dispermic) and no maternal chromosomes. CHMs affect approximately 1 in every 1,400 pregnancies.[1] Among androgenetic CHMs (AnCHMs), monospermic ones account for 85% of the cases and dispermic ones for 15% of the cases.[2] Androgenetic monospermic CHMs were first described in 1977,[3] but the proposed mechanisms of their occurrence remained hypothetical. It is believed that after fertilization between a haploid sperm and an oocyte that has lost its nuclear DNA (for simplicity referred hereafter as empty oocyte), the paternal genome endoduplicates to reconstitute diploidy. Then, because the paternal and maternal genomes have different roles in cellular proliferation and embryonic differentiation, the androgenetic genome that results from such a zygote leads to the molar phenotype. However, in decades of *in vitro* fertilization, no one has seen or reported individuals who produced systematically empty oocytes.[4] A new mechanism for the origin of AnCHMs was suggested: that dispermic fertilization of a haploid oocyte followed by postzygotic diploidization is more likely to be at the origin of the different genotypic types of sporadic HMs as well as of their association with mosaicisms and twin pregnancies consisting of one fetus with a normal placenta and a HM.[4]

Recurrent HMs (RHMs) affect 1.5%–9% of women with a prior HM.[5–10] There are two genes, *NLRP7* (MIM: 609661)[11] and *KHDC3L* (MIM: 611687),[12] responsible for RHMs. Bi-allelic mutations in these two genes explain the etiology of RHMs in 60% of affected women.[13] Recurrent molar tissues from women with bi-allelic mutations in the two known genes are all diploid biparental while those from women without mutations are heterogeneous. Among women with no recessive mutations in the known genes, a minority of women have diploid biparental RHMs, half of the remaining women have triploid dispermic

[1]Department of Human Genetics, McGill University Health Centre, Montréal, QC H4A 3J1, Canada; [2]Genome Québec Innovation Center, Montréal, QC H3A 0G1, Canada; [3]Department of Obstetrics and Gynecology, Gynecologic Oncology Division, Centre Hospitalier de l'Université de Montréal, Réseau des Maladies Trophoblastiques du Québec, Montréal, QC H2X 0C1, Canada; [4]Department of Obstetrics & Gynecology, Post Graduate Institute of Medical, Education and Research, PGIMER, Chandigarh 160012, India; [5]Department of Medical Genetics, Faculty of Medicine, Baskent University, 06810 Ankara, Turkey; [6]Department of Obstetrics and Gynecology, Baylor College of Medicine, Houston, TX 77030, USA; [7]Department of Pathology, Centre Hospitalier de l'Université de Montréal, Montréal, QC H2X 0C1, Canada; [8]Ovo Clinic, Montréal, QC H4P 2S4, Canada; [9]Department of Obstetrics and Gynecology, Centre Hospitalier de l'Université de Montréal, Montréal, QC H2X 0C1, Canada; [10]Invitae, Irvine, CA 92618, USA; [11]Cytology & Gynecological Pathology, Post Graduate Institute of Medical Education and Research PGIMER, Chandigarh 160012, India; [12]Department of Obstetrics and Gynecology, McGill University Health Centre, Montréal, QC H4A 3J1, Canada; [13]Department of Surgery, McGill University Health Centre, Montréal, QC H4A 3J1, Canada; [14]Department of Biology, McGill University, Montréal, QC H3A 0G4, Canada
[15]These authors contributed equally to this work
*Correspondence: rima.slim@muhc.mcgill.ca
https://doi.org/10.1016/j.ajhg.2018.10.007.

PHMs, and the second half have androgenetic monospermic CHMs.[13] Available data on women with diploid androgenetic monospermic RHMs indicate that 17%–37% of them fail to have live births, suggesting that these women may have a strong genetic defect underlying their RHMs.[13,14]

To identify mutations responsible for RHMs, we performed whole-exome sequencing (WES) on a total of 65 women with RHMs (including all histopathological and genotypic types), miscarriages, and infertility, who were negative for mutations in *NLRP7* and *KHDC3L*. We identified bi-allelic deleterious mutations in meiotic double-stranded break formation protein 1 (*MEI1*) (MIM: 608797), type 2 DNA topoisomerase 6 subunit B-like (*TOP6BL*/*C11orf80*) (MIM: 616109), and REC114 meiotic recombination (*REC114*) genes in five unrelated women, of which two had other family members with recurrent miscarriages and infertility. We demonstrated that their HMs have the histopathological features of CHMs and have androgenetic monospermic genomes. All three genes are conserved during evolution and are known to play roles during early homologous chromosome pairing and recombination in the mouse oocyte.[15–17] *In vitro* maturation of oocytes from *Mei1*-deficient female mice has previously been reported, but the number of obtained mature oocytes was very small and consequently, mature oocytes were not further examined.[15] In the current study, we focused on the segregation of chromosomes at the first meiotic division and the possibility of androgenetic embryonic development. We confirm that most $Mei1^{-/-}$ oocytes have abnormal spindle morphology and misaligned chromosomes on the spindles, and 63% of them fail to extrude the first polar body (PB). However, 20% of oocytes extruded morphologically abnormal first PB and some extruded all their chromosomes together with the spindle microtubules into the PB and were empty with no chromosomes. We demonstrate that $Mei1^{-/-}$ oocytes are capable of fertilization and that 5% lead to androgenetic zygotes. We finally show that the zygotes derived from *Mei1*-deficient oocytes are capable of initiating embryonic development but mostly arrest at the 2- to 4-cell stage.

Material and Methods

Subjects

Written informed consents were obtained from all participants and the study was performed accordance to the McGill University Research Ethics guidelines (Institutional Review Board # A01-M07-98 03A). Blood or saliva from affected women and their family members were collected. Genomic DNA was isolated from whole blood cells using Flexigene DNA Kit (QIAGEN). The products of conception from different pathology laboratories were retrieved for genotype analysis.

Mutation Analyses

Mutation analyses of *NLRP7* and *KHDC3L* were performed to exclude the presence of mutations in these two genes before sending for whole-exome sequencing. PCR conditions and the sequences of primers were previously described and samples were sent for Sanger sequencing in both directions.[11]

Whole-Exome Sequencing

Whole-exome library preparation, capturing, sequencing, and bioinformatics analyses were carried out at the McGill University and Genome Quebec Innovation Center, Montreal, Canada as previously described.[18] Whole exome was captured using either SureSelect Human All Exon Kit version 5 (Agilent Technologies) or the Roche Nimblegen SeqCap EZ Human Exome capture kit on 3 μg or 500 ng gnomic DNA, respectively, and sequenced on an Illumina HiSeq 2000 sequencer with paired-end 100-base pair reads. The paired-end sequences were trimmed and aligned to the human reference genome hg19 using BWA (v.0.5.9).[19] The Genome Analysis Toolkit (GATK)[20] was used to perform local realignment around small insertions and deletions (indels) and to assess capture efficiency and coverage for all samples. The latter was calculated after marking duplicate reads by Picard. Variants were called individually for each individual using Samtools (v.0.1.17)[21] and annotated by Annovar.[22] Subsequently, several filtering criteria were applied to prioritize the potential causal variants from non-pathogenic polymorphisms and sequence errors. The variants were excluded when they were seen at a minor allele frequency (MAF) greater than 0.01 in public databases (ExAC, 1000 Genomes, NHLBI exome databases) or in-house exomes database (>1,000 exomes). Finally, only the most likely damaging variants (nonsense, canonical splice-site, conserved missense, and coding indels) were considered and manually examined in IGV[23] if they were predicted to be deleterious by at least two bioinformatics algorithms (PolyPhen, SIFT, MutationTaster, CADD-Combined Annotation Dependent Depletion).

Sanger Sequencing Validation of Identified Mutations

Sanger sequencing was used to validate the mutations identified by exome sequencing and to check the segregation of the mutations in other family members. Primers were designed using Primer Blast. PCR conditions and sequences of the primers are provided in Table S1. Variant nomenclature is provided according to the GenBank references for *MEI1* (GenBank: NM_152513.3 and NP_689726.3), for *TOP6BL/C11orf80* (GenBank: NM_024650.3 and NP_078926.3), and for *REC114* (GenBank: NM_001042367.1 and NP_001035826.1).

Targeted Sequencing

The candidate genes were screened in additional affected women with milder phenotypes (Table S3). *MEI1* and *REC114* were screened in 99 affected women (of which 53 had at least 1 HM and the remaining had ≥3 miscarriages). *TOP6BL/C11orf80* was screened in 246 affected women (46 women with at least 1 HM and the remaining had ≥3 miscarriages).

RT-PCR on Lymphoblastoid Cell Line and Human Oocytes

RNA was extracted from EBV-transformed lymphoblastoid cell line (LCL) from affected women and controls using Trizol (Invitrogen). Human oocytes at different stages (total 4–8 oocytes each stage) were obtained from women undergoing IVF/ICSI and were collected by removing the zona pellucida with acidified Tyrode's solution and washed in 1× PBS before putting them in lysis buffer as previously described.[24] cDNA synthesis was performed using a

reverse transcription kit (Life Technologies, Thermo Scientific). PCR conditions and primers for RT-PCR are provided in Table S1.

H&E Staining, p57^{KIP2} Immunohistochemistry, Flow Cytometry, Microsatellite Genotyping, and SNP Microarray Analysis

Sections of formalin-fixed, paraffin-embedded (FFPE) tissues were prepared for H&E staining, p57^{KIP2} immunohistochemistry, flow cytometry, and microsatellite genotyping as previously described.[13] Microarray analysis search for aneuploidies in products of conception of affected women was performed at Invitae as previously described.[25]

Mice

Mei1 heterozygous mice (B6.129S1-Mei1m1Jcs/Mmnc)[26] were purchased from the MMRRC (Mutant Mouse Resource & Research Centers Supported by NIH, USA) (MMRRC#31721), maintained on the C57BL/6J background (Jackson Laboratory), and crossed to produce homozygous null *Mei1*. Genotyping was done according to the MMRRC protocol. The mice were fed in a temperature- and light-controlled room at the Animal Resource Division of the McGill University Health Centre Research Institute. All the procedures and ethics were approved by the McGill University Animal Care Committee in accordance with the Canadian Council on Animal Care. Food and water were provided *ad libitum*.

RT-PCR on Mouse Tissues

Ovaries, germinal vesicle-stage (GV) oocytes, and metaphase II (MII) oocytes (total of 70–100 oocytes) were collected from 12.5 dpc (days postcoitum), 17.5 dpc, newborn, 5 dpp (days postpartum), and adult wild-type females. Total RNA was extracted using the RNeasy plus Micro and Mini Kit (QIAGEN) according to the manufacturer's instructions. cDNA was synthesized (Invitrogen) and used as template for RT-PCR. β-actin was used as a control. The primers and conditions used for RT-PCR are provided in Table S2. The transcript levels of genes were checked using 2% agarose gel.

Mouse Oocyte Maturation *In Vitro* and *In Vivo*

For *in vitro* oocyte maturation, female mice at 25–27 dpp were intraperitoneally injected with 10 IU eCG (equine chorionic gonadotropin) per mouse. The mice were killed by cervical dislocation 46–48 hr later and the ovaries were collected to retrieve cumulus cell-oocyte complexes (COCs). COCs were cultured in α-MEM medium containing 5 IU/mL FSH (follicle-stimulating hormone, Sigma), 5% HI-FBS (heat inactivated fetal bovine serum), 7.5 μL/mL 100× penicillin/streptomycin, and 0.25 mM sodium pyruvate (GIBCO, Thermo-Fisher Sci) for 17 to 19 hr for all experiments[27] except for the experiment to assess meiotic progression and delay. For this experiment, maturation was extended to 24 hr of *in vitro* culture. For *in vivo* oocyte maturation, females at 25–27 dpp were intraperitoneally injected with 10 IU eCG, and 46–48 hr later, with 7.5 IU hCG (human chorionic gonadotropin; Sigma) per mouse. 15 hr later, oocytes were collected from oviduct ampullae.

Mouse Embryo Culture *In Vitro*

Hormonal treatment with dCG followed by hCG was done as described above at 25–27 dpp and the females were left with DBA/2 males (Charles River Laboratories) overnight. 20 hr after hCG injection, zygotes were collected from oviduct ampullae and cumulus cells were removed using 1% hyaluronidase. Washed zygotes were used for immunofluorescence staining or cultured in KSOM (Millipore) for 5 days under 5% CO_2 with humidity at 37°C. Embryo development was recorded daily.

Immunofluorescence

Immunofluorescence staining was carried out as previously described.[28] Briefly, oocytes were fixed in 4% paraformaldehyde (PFA) in PBS for 30 min and then transferred to membrane permeabilization solution (0.5% Triton X-100) in water for 20 min. Thereafter, oocytes were blocked in 1% BSA (bovine serum albumin) in PBS for 1 hr. The oocytes were then incubated with primary antibodies diluted with 1% BSA overnight at 4°C. After incubation with secondary antibodies at room temperature for 1 hr, oocytes were placed in mounting medium with DAPI (Vector). Fluorescence was visualized using Zeiss LSM780 Scanning Confocal Microscope at the Molecular Imaging Facility of the Research Institute of the McGill University Health Centre.

Antibodies

The following antibodies were used; mouse-anti-H3K9me2 (1:50, Abcam), mouse-anti-α-tubulin (1:100, Santa Cruz), and donkey-anti-mouse IgG-Alexa fluor 488 (1:500, Invitrogen).

Live Imaging

COCs were cultured for maturation in α-MEM as previous described for 12 hr, and then cumulus cells were removed using 1% hyaluronidase. The denuded oocytes were incubated with 5 ng/mL Hoechst 33342 in α-MEM supplemented as above without FSH for 30 min. Thereafter, the oocytes were transferred to Zeiss LSM780 Scanning Confocal Microscope to monitor the first polar body extrusion, by scanning every 20 min, for 7 hr.

Results

Identification of Bi-allelic Mutations in *MEI1*, *TOP6BL*/*C11orf80*, and *REC114*

We performed WES on 65 women with RHMs (including all histopathological and genotypic types) and without mutations in *NLRP7* or *KHDC3L* and 18 of their relatives. After aligning the WES reads to the reference genome, variants-calling, and filtering for rare variants with minor-allele frequency < 0.01, we analyzed the data under the recessive mode of inheritance because of its compatibility with the inheritance of the disease in all reported cases of RHMs (with or without mutations in the two known genes). We identified rare bi-allelic deleterious mutations (nonsense, canonical splice-site, evolutionary conserved missense, and coding indel) in seven important candidate genes. We next performed targeted sequencing of the seven candidate genes on 99 to 246 women with milder defects (2 HMs or ≥ 3 miscarriages with or without 1 HM) (from all genotypic types) (Table S3). The two approaches led to the identification of bi-allelic potentially deleterious mutations in three genes in five unrelated affected women, including two from familial cases.

In *MEI1*, exome sequencing revealed a novel homozygous protein-truncating mutation in exon 28, c.3452G>A

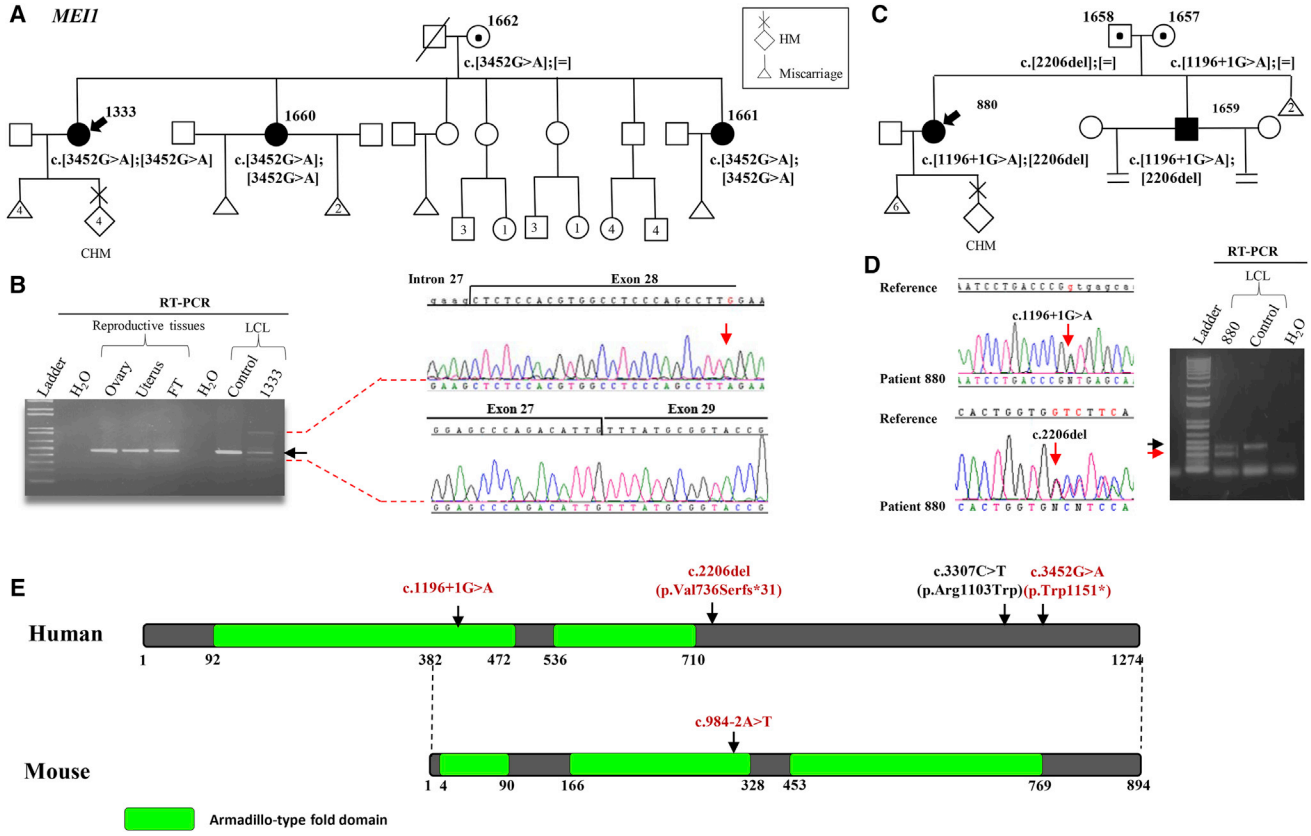

Figure 1. Pedigree Structure, Reproductive Outcomes, and Mutation Analysis of Two Families with Bi-allelic *MEI1* Mutations
(A) Sanger sequencing and segregation of the mutation identified in *MEI1* in the family of proband 1333 (indicated by an arrow).
(B) RT-PCR demonstrating abnormal splicing caused by the nonsense mutation (c.3452G>A) and the generation of three cDNA fragments, the normal fragment indicated by a black arrow and two abnormal fragments indicated by dashed red lines (a larger fragment that includes intron 27 and a smaller fragment that skips exon 28).
(C) Sanger sequencing and segregation of the mutations identified in *MEI1* in the family of proband 880 (indicated by an arrow).
(D) Abnormal splicing in affected individual 880 showing the amplification of a smaller cDNA fragment that corresponds to the skipping of exon 11 (red arrow) and another cDNA fragment corresponding to the normal splicing isoform (black arrow). RNA was from lymphoblastoid cell lines (LCL) of the affected women.
(E) Schematic presentation of the domains of human and mouse MEI1. The positions of the mutations are indicated by arrows. The mutations identified in this study are shown in red. In black is a recently reported mutation in two infertile brothers with non-obstructive azoospermia. The mutation in the *Mei1* knockout is shown on the mouse protein.

(p.Trp1151*), in proband 1333 (Figure 1A, Table S4) with a history of four miscarriages followed by four HMs, all from spontaneous conceptions. In addition, she had one failed cycle of *in vitro* fertilization by intra-cytoplasmic sperm injection (Table S5). Analyzing additional samples from other family members identified the same mutation in a homozygous state in two sisters who had one and three miscarriages, respectively, and both underwent total abdominal hysterectomy because of several uterine fibroids. The mother of the three sisters was found to be a heterozygous carrier of their mutation (Figure 1A). Using RT-PCR on total RNA from a lymphoblastoid cell line (LCL) from the proband 1333, we found that the mutation leads to, in addition to the normal splicing isoform, two abnormal splicing isoforms: a larger cDNA fragment caused by the insertion of intron 27 between exons 27 and 28 and a smaller cDNA fragment due to the skipping of exon 28 (Figure 1B). This aberrant splicing was seen only in the affected woman and not in control subjects and is most likely mediated by the nonsense-mediated decay.[29,30]

The second family consists of a woman (proband 880) with six miscarriages and one CHM and her brother, who is infertile, with non-obstructive azoospermia and no Y chromosome deletions. Both were found compound heterozygous for an invariant splice site mutation, c.1196+1G>A, affecting the splice donor of exon 10, and a 1-bp deletion, c.2206del (p.Val736Serfs*31), in exon 19 (Figure 1C, Table S4). The two mutations segregated in the family, one from each parent. Using RT-PCR on total RNA from a LCL from the proband 880, we found that the invariant splice site mutation, c.1196+1G>A, leads to a smaller cDNA fragment that corresponds to the skipping of exon 11 (Figure 1D) located in one of the two predicted Armadillo-type fold domains (Figure 1E). These two mutations were identified in proband 880 by targeted

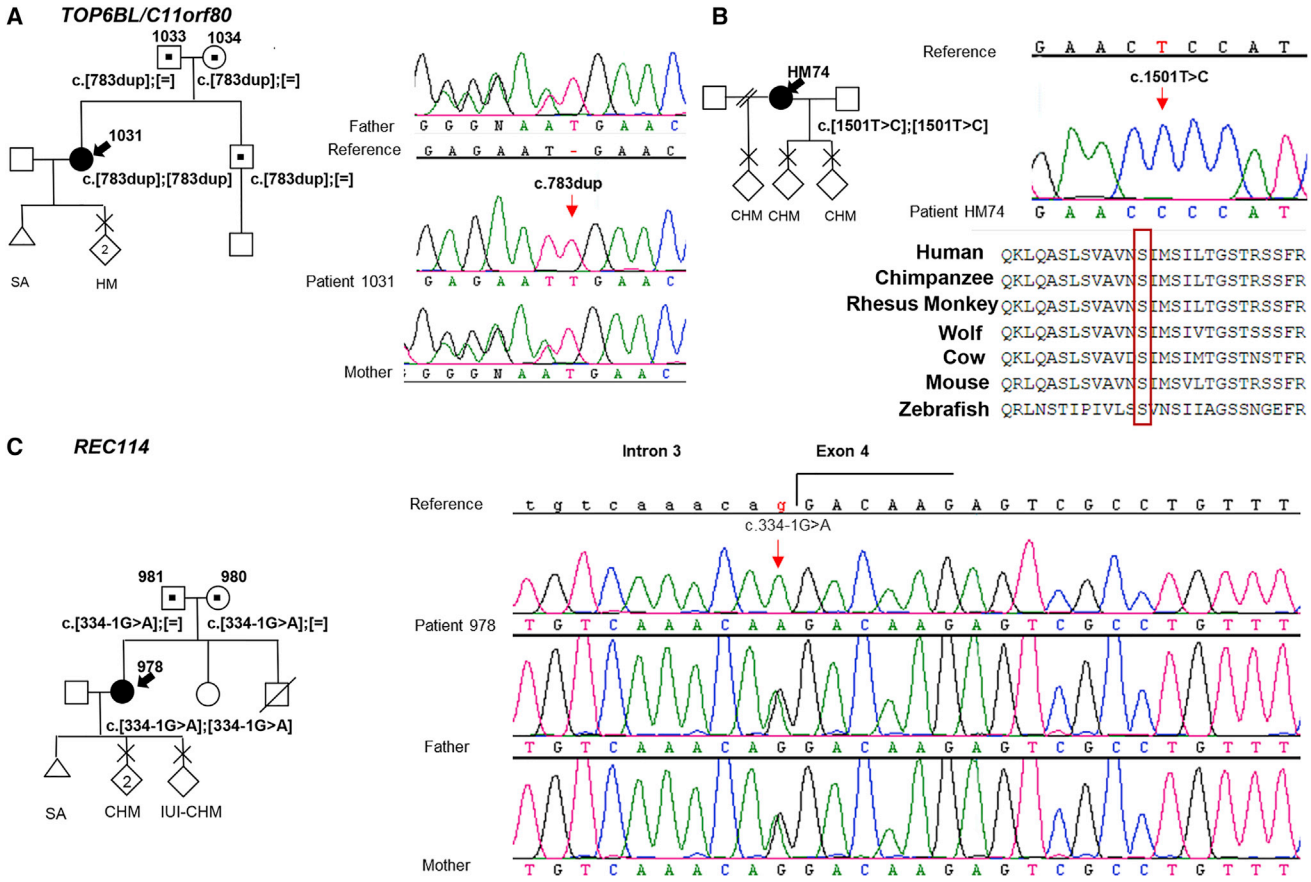

Figure 2. Pedigree Structure, Reproductive Outcomes, and Mutation Analyses of *TOP6BL/ C11orf80* and *REC114* in Three Affected Women with Bi-allelic Mutations

(A) Pedigree of proband 1031 showing the segregation of *TOP6BL/C11orf80* mutations and the chromatograms.

(B) Pedigree of proband HM74 showing the chromatogram of her mutation in *TOP6BL/C11orf80* and the conservation of the changed amino acid in different species by multiple alignment from NCBI.

(C) Pedigree of proband 978 with *REC114* mutation and the chromatograms.

sequencing and then in her other family members by Sanger sequencing.

In *TOP6BL/C11orf80*, we found in one woman (ID 1031), with one miscarriage and two HMs, a 1-bp insertion, c.783dup (p.Glu262*) in a homozygous state (Figure 2A, Table S4). The mutation segregated from both parents who were found to be heterozygous carriers. In a second woman with RHMs (ID HM74, previously reported as the affected woman 2[31]), we found a homozygous missense variant c.1501T>C (p.Ser501Pro) that affects a highly conserved amino acid (PolyPhen = 0.9, CADD = 22.5) (Figure 2B, Table S4). The c.783dup mutation leads to the truncation of the protein before the transducer domain. The second mutation, c.1501T>C (p.Ser501Pro), affects a conserved amino acid residue also involved in the interaction of TOP6BL transducer domain with SPO11, a component of topoisomerase 6 complex required for the formation of double-strand breaks in mice.[16] These two mutations in *TOP6BL* were identified by exome sequencing.

In *REC114*, using exome sequencing, we found in one woman (ID 978) with a miscarriage and three CHMs a novel splice acceptor mutation, c.334−1G>A, in a homozygous state (Figure 2C, Table S4). Of note that the last CHM of this woman was conceived with the help of intrauterine insemination because of her infertility. We did not detect *REC114* transcripts in LCL and consequently could not check the effect of this mutation on gene splicing. The mutation segregated in the family and the two parents were found to be heterozygous carriers (Figure 2C).

MEI1, *TOP6BL/C11orf80*, and *REC114* are conserved from yeast to human and their functions have been examined in several organisms including yeast,[31,32] plants,[33] worms,[34] and mice.[15–17] It was striking to see that all three genes play a key role in the formation of double-strand breaks, which is essential for homologous chromosome synapsis and recombination during meiosis I. Mutations in these three genes have never been reported in any human disease with the exception of a recent case of two infertile brothers with a homozygous bi-allelic *MEI1* mutation.[35] Therefore, the presence of bi-allelic mutations in five unrelated women and three affected siblings establishes their causal role in recurrent HMs and miscarriages, and in male and female infertility in humans.

Affected Women with Bi-allelic *MEI1* Mutations Have AnCHMs

We next retrieved all HM tissues from affected women 1333 and 880 with *MEI1* mutations and comprehensively analyzed them. By morphological evaluation, all tissues fulfilled the histopathological criteria of CHMs, did not express $p57^{KIP2}$ in the nuclei of the cytotrophoblast and villous mesenchyme cells, were diploid by flow cytometry, androgenetic monospermic by microsatellite DNA markers genotyping, and did not have aneuploidies by SNP microarrays (Figures S1–S4). Two CHM tissues from affected woman 978, with bi-allelic *REC114* mutations, were genotyped by the referring laboratory and found androgenetic monospermic. The tissues from affected woman HM74, with bi-allelic mutations in *TOP6BL*/*C11orf80*, were reported to be most likely androgenetic CHMs.[36] Therefore, HMs from affected women with mutations in the three genes are androgenetic and have a different mechanism at their origin than HMs from women with bi-allelic mutations in *NLRP7* or *KHDC3L*.

A complete hCG follow up after HM evacuation was available for affected women 880 and 1031 and both had low risk persistent trophoblastic diseases after the last conception. The non-molar miscarriages of all affected women with mutations in the three genes did not require dilatation and curettage and therefore are not available for evaluation.

Taken together, these data indicate that the bi-allelic mutations in three genes we identified may not be responsible only for recurrent androgenetic CHMs, but also for recurrent miscarriages and female and male infertility.

Expression of *Mei1*, *Top6bl* /*C11orf80*, and *Rec114*

In humans, the three genes are transcribed in ovaries and some other somatic tissues (Figures 1B and S5A) but were not detected in oocytes (4–8 oocytes per sample). In mice, the three genes were detected in ovaries from embryonic day 12 to 5 days postpartum (dpp) (Figure S5B), and these data are in agreement with a previous report.[26] While *Top6bl* and *Rec114* were found expressed in germinal vesicles (GV) and metaphase II (MII) oocytes from 25 dpp mice, *Mei1* expression was not detectable in GV or MII mouse oocytes (70–100 oocytes per sample).

Evidence of Empty Oocytes from Null *Mei1* Females

In humans, it is unknown how an androgenetic monospermic CHM forms and such an entity has never been reported in animals. To elucidate the mechanism(s) leading to androgenetic monospermic CHM and possibly model some of its features in mice, we used a mouse knockout for *Mei1* that was available when we identified the mutations in the affected women.[15] The mutation in the *Mei1* knockout (c.984−2A>T) is very close to one of the mutations, p.Val736Serfs*31, found in proband 880 (Figure 1E), and results in two abnormal splice isoforms which are predicted to lead to premature stop codons. $Mei1^{-/-}$ males and females are infertile, but otherwise healthy.[15] While the males have no spermatozoa in their testes, the females have oocytes in all follicular stages at young ages, albeit in reduced numbers. The development of oocytes during *in vitro* maturation has been reported for $Mei1^{-/-}$ and it was found that 94% of the oocytes arrest at metaphase I and have abnormal spindles with misaligned chromosomes scattered on the spindles; only 6% of $Mei1^{-/-}$ oocytes progress to metaphase II and extrude the first PB. To better understand the mechanism of AnCHM formation, we compared the development of oocytes from $Mei1^{-/-}$ with those of wild-type after *in vitro* maturation. Under our experimental conditions of *in vitro* maturation for 17–24 hr, we found that oocytes from $Mei1^{-/-}$ have delayed meiotic progression (Figure 3A). We found that 96% of oocytes from the wild-type and only 8% of oocytes from $Mei1^{-/-}$ extruded the first PB of normal size and shape. However, 63% of oocytes from $Mei1^{-/-}$ failed to extrude the first PB; 20% extruded abnormal PB, either one PB of normal size and with a rough surface, one large PB, or two PBs (despite not being fertilized); the remaining 6% of oocytes appeared to be 2- to 4-cell-like or degenerating (Figures 3B–3D). These PB abnormalities were also observed in *in vivo* matured $Mei1^{-/-}$ oocytes (Figure 3D) with the exception that more oocytes were seen without PB in both mutant and wild-type, probably because the first PB had degenerated, a well-documented phenomenon of *in vivo* maturation.[37]

We next examined the spindle morphology and chromosome congregation in the *in vitro* matured oocytes using immunofluorescence localization of α-tubulin and DAPI staining of the chromosomes. We found that all oocytes without PB had chromosomes, but the chromosomes were misaligned on the spindles of abnormal shapes (Figure 4B). Of the oocytes that extruded PB, approximately 70% appeared at telophase, i.e., the spindles were seen between the two sets of chromosomes without clear separation between the oocytes and the PB. Some oocytes with two PBs had tripolar spindles with chromosomes at each pole and two of them forming two first PBs (Figures 4C and 4D). Other oocytes had bipolar spindles with chromosomes at both ends, but both the spindles and the chromosomes at their poles were altogether extruded into the first PB leaving the oocytes with few chromosomes (Figure S6) or empty with no chromosomes (Figures 4D–4F). Empty oocytes were also observed in *in vivo* matured oocytes (Figure S7). Such empty oocytes were observed only among those that extruded abnormal PB and accounted for approximately 8% of oocytes with ≥1 PB matured *in vitro* or *in vivo*. Empty oocytes were not observed in wild-type or $Mei1^{+/-}$ mice after either *in vitro* or *in vivo* maturation. In addition, we did not see spindles or chromosomes congregation abnormalities in oocytes from $Mei1^{+/-}$, which behaved like those from wild-type mice. Using live imaging, we monitored *in vitro* maturation of oocytes from $Mei1^{-/-}$ and confirmed the extrusion of all the chromosomes into the PB in some oocytes (Video S1).

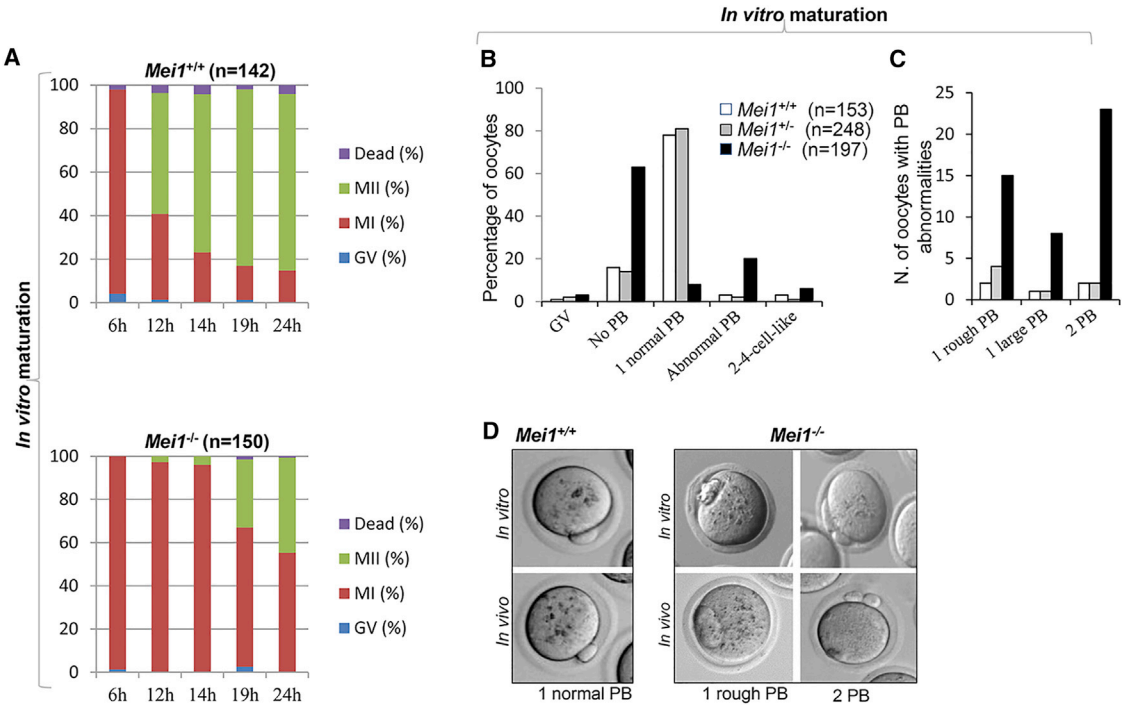

Figure 3. Meiosis I Abnormalities in Oocytes from Wild-Type, Heterozygous, and Homozygous Mice
(A) Fully grown oocytes from *Mei1*$^{+/+}$ and *Mei1*$^{-/-}$ mice were cultured *in vitro* and the frequency of various stages at different time point were recorded by phase contrast microscopy. The absence of polar body (PB) 17–19 hr after germinal vesicle (GV) breakdown was our criterion for arrest before metaphase I stage (MI) and the presence of at least one PB was our criterion for progression to metaphase II arrest (MII).
(B) Percentages of oocytes with or without abnormalities observed after *in vitro* maturation.
(C) Numbers (N) of oocytes with various PB abnormalities observed after *in vitro* maturation.
(D) Examples of oocytes with abnormal polar bodies after *in vitro* or *in vivo* maturation.

Evidence of Androgenetic Zygotes from Null *Mei1* Oocytes

We next asked whether oocytes from null *Mei1*$^{-/-}$ are capable of fertilization. Because the rate of fertilization and embryonic development *in vitro* is lower than *in vivo*, we used superovulation and natural mating in all subsequent experiments of embryonic development. To distinguish maternal from paternal chromosomes in the zygotes, we used immunofluorescence with an antibody against dimethylated histone 3 at lysine 9 (H3K9me2). H3K9me2 is an epigenetic marker that is acquired during oogenesis, but not during spermatogenesis; consequently, it distinguishes maternal from paternal chromosomes up to pronuclear fusion in late zygotes.[38] We first confirmed similar immunofluorescence staining of H3K9me2 between wild-type and *Mei1*$^{-/-}$ oocytes at GV to MII stages (Figure 5A). We next examined the oocytes after fertilization and confirmed that H3K9me2 stains only the maternal but not paternal chromosomes in control zygote (Figure S8). Among the 113 oocytes from *Mei1*$^{-/-}$ females analyzed, 68 (60%) had evidence of fertilization and contained paternal DNA. Some zygotes were penetrated by cumulus cells (Figures S9 and S10) and such zygotes were fertilized by two or three spermatozoids. Among all the zygotes, approximately 5% were androgenetic and did not contain maternal chromosomes. Figure 5B shows a zygote that had lost all maternal DNA into the PB (positive for anti-H3K9me2) and started the first mitotic division of the male pronucleus. All z axis stack sections of this zygote are shown in Video S2. We also observed zygotes that had retained very few maternal chromosomes and others that had undergone asymmetrical cleavage into 2-cell-like, with one cell containing paternal pronucleus or sperm head and the other containing maternal pronucleus (Figure S11).

Zygotes from Null *Mei1* Oocytes Can Initiate Embryonic Development

We next investigated whether the zygotes derived from *Mei1*$^{-/-}$ oocytes can initiate embryonic development. We crossed *Mei1*$^{-/-}$ females with wild-type males overnight, collected oocytes, and monitored their daily development in culture for up to 5 days using phase contrast microscopy (Figure 6). Our analysis demonstrated that 72% of embryos (n = 200) derived from *Mei1*$^{-/-}$ females underwent cleavage, but most were arrested at the 2-cell or 4-cell stage, only 2% reached the blastocyst stage after 120 hr post-fertilization, and none hatched (Figure 6). For comparison, 78% of oocytes from wild-type mice reached the blastocyst stage 96 hr post-fertilization and all hatched. In conclusion, oocytes from *Mei1*$^{-/-}$ females can be fertilized and undergo embryonic development but their chance to

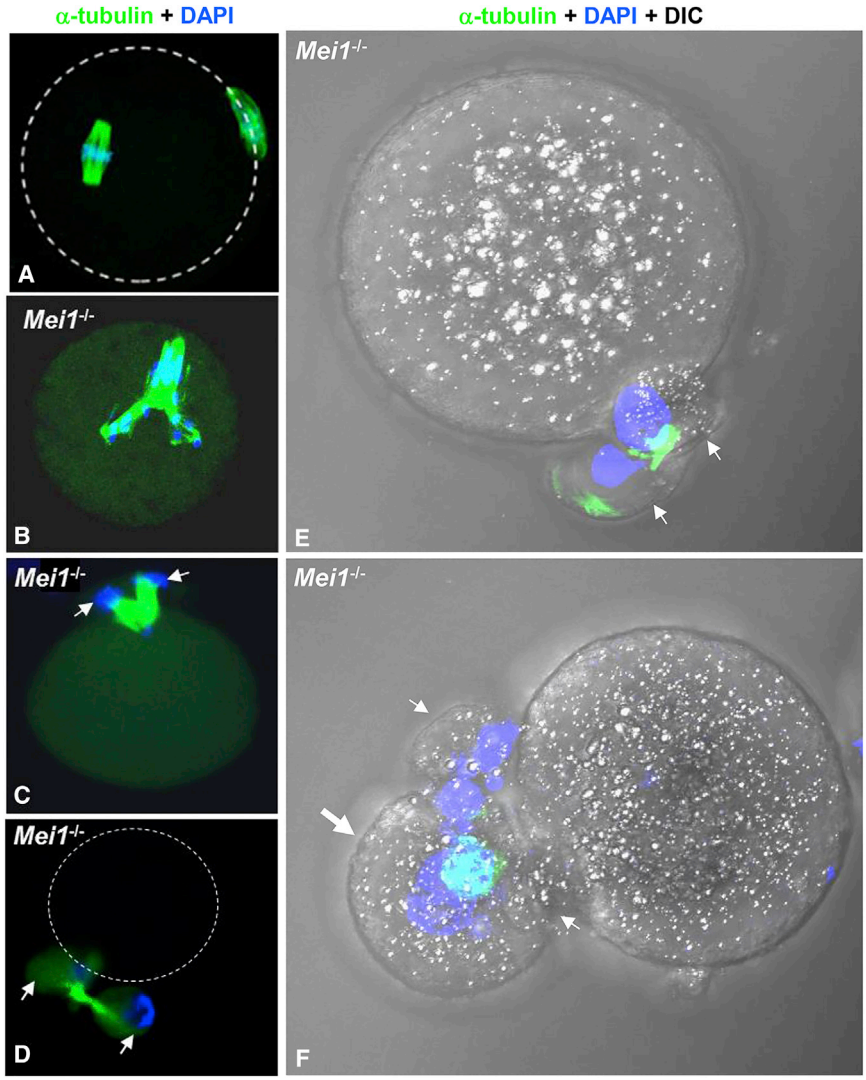

Figure 4. Various Spindle and Chromosome Congression Abnormalities after *In Vitro* Maturation

(A) Oocyte from wild-type at MII displaying two normal spindles, one in the oocyte with aligned chromosomes and another in the polar body (PB).

(B) An oocyte from *Mei1*$^{-/-}$ with tripolar spindles within the oocyte and misaligned chromosomes.

(C) An oocyte from *Mei1*$^{-/-}$ with tripolar spindles that had extruded DNA at two poles into the PB (arrows).

(D) An empty oocyte from *Mei1*$^{-/-}$ that had extruded the spindles and the chromosomes at their two poles into two PB (arrows).

(E) Another empty oocyte from *Mei1*$^{-/-}$ that had extruded all its DNA with the spindles into the PB (arrows).

(F) An oocyte that extruded one large (large arrow) and two normal-size PB (small arrows).

reach the stage for implantation is limited. Their development in uterus or on the genetic background other than C57/B6 remains an open question.

Discussion

Here we provide evidence implicating bi-allelic mutations in three genes, *MEI1*, *TOP6BL*, and *REC114*, in the causation of recurrent androgenetic monospermic hydatidiform moles, miscarriages, and infertility in humans. This evidence is based on the identification of bi-allelic mutations in *MEI1* in two familial case subjects, in *TOP6BL* in two unrelated women, and in *REC114* in one woman. The implication of *REC114* is also based on the known interaction of its protein with MEI4, an interactor of MEI1 in yeast and mice.[17,32] These three genes have been studied in various organisms and model systems and all are required for double-strand breaks formation in the early phase of meiosis in oocytes. Analyzing five HMs from two unrelated women with *MEI1* mutations demonstrated that the five tissues fulfill the histopathological criteria of CHMs, lack p57^{KIP2} expression, and have diploid androgenetic monospermic genomes. Tissues from proband 978 with mutations in *REC114* were referred to us as androgenetic monospermic CHMs and those from woman HM74, with mutations in *TOP6BL*, are believed to be androgenetic CHMs. Taken together, these data establish the role of *MEI1*, and possibly the two other genes, in the genesis of androgenetic CHMs.

Among the three identified genes, *Mei1* is the most studied and its functional role has been investigated in several species,[15,31,33,34] of which mouse is the closest, evolutionarily, to human. Null mouse mutants fail to complete the first meiotic division due to defective double-strand breaks formation. *MEI1* was the first of the three genes, in which we found mutations in two unrelated families, and we were able to access the HM tissues and demonstrate their androgenetic monospermic genomes, so we set out to investigate whether androgenetic pregnancies or conceptions occur in *Mei1*-null mice. Because *Mei1*-null female mice were documented to be infertile, we hypothesized that perhaps androgenesis occurs in them but such conceptions do not implant and lead to detectable pregnancies. We asked three main questions. (1) Do *Mei1*-deficient females produce empty oocytes with no maternal chromosomes? (2) When do *Mei1*-deficient oocytes lose their chromosomes, before or after fertilization? (3) By which mechanism do *Mei1*-deficient oocytes lose their chromosomes? To answer these questions, we followed the development of oocytes from null *Mei1* in *in vitro* maturation. We found that 8% of *Mei1*$^{-/-}$

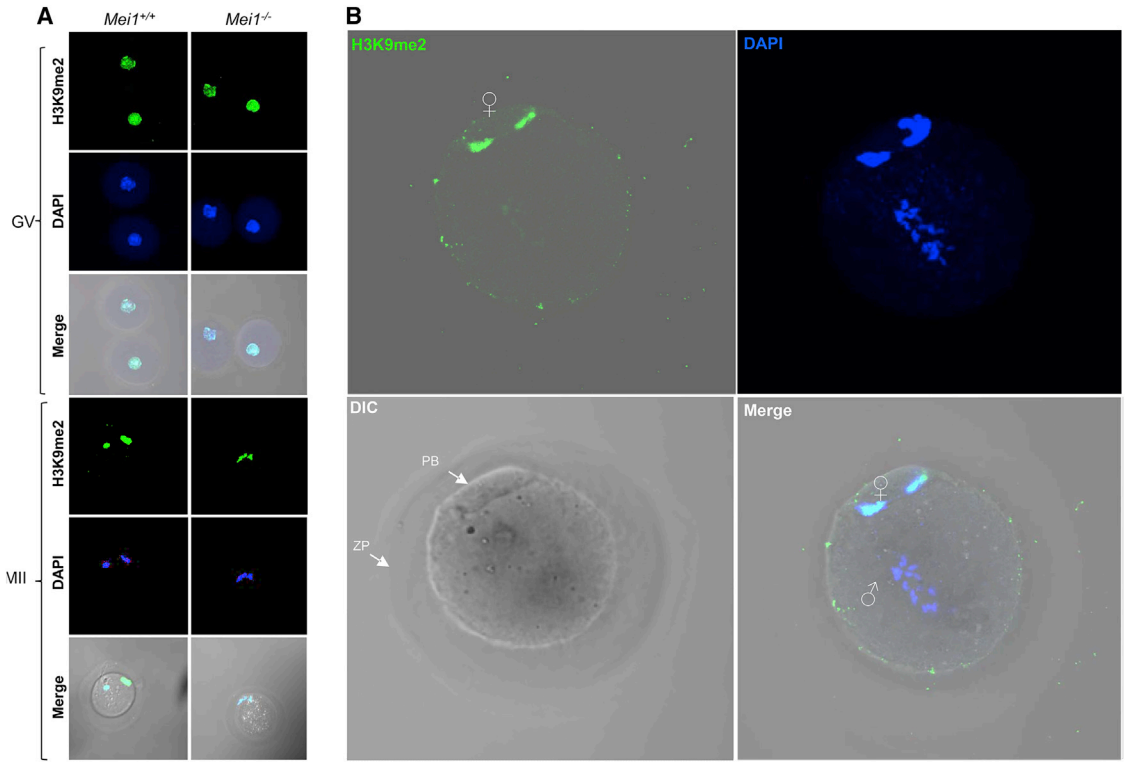

Figure 5. H3K9me2 Staining of Maternal Chromosomes in Oocytes and Zygotes from Wild-Type and *Mei1*$^{-/-}$
(A) H3K9me2 immunofluorescence of GV and MII oocytes from wild-type and *Mei1*$^{-/-}$ females, demonstrating that H3 methylase is not impaired in *Mei1*-deficient oocytes.
(B) H3K9me2 immunofluorescence on zygotes showing the staining of maternal but not paternal chromosomes in a zygote from *Mei1*$^{-/-}$ females. GV stands for germinal vesicle; MII, metaphase II; PB, polar body; ZP, zona pellucida; ♀, maternal chromosomes; ♂, paternal chromosomes; and DIC, differential interference contrast.

extruded all their chromosomes together with the spindles into the first PB. Our results are in agreement with some observations made on null *mei1* in *C. elegans*, which either fail to produce PBs, produce PBs with variable numbers of maternal chromosomes, or produce large PBs appearing to contain all maternal chromosomes.[34,39] Furthermore, we showed that the oocytes from *Mei1*-null females can be fertilized and 5% of the zygotes had lost all their maternal chromosomes into the PBs, and were therefore androgenetic. In addition, some of the zygotes retained very few maternal chromosomes, which may be unable to fuse with the paternal pronucleus and result also in androgenetic embryos. From our analysis, another potential mechanism that would lead to androgenesis may occur during postzygotic cleavage of a fertilized nucleated oocyte, resulting in the separation of paternal DNA into one cell and maternal DNA into another (Figure S11). Such aberrant cells with different genomes may have different growth rates, be subject to some selection, and lead to mosaic conceptions including AnCHMs. However, based on our observations, such events are unlikely to be at the origin of RHMs in women with *MEI1* mutations because they were not recurrent in *Mei1*-deficient females. Some of the androgenetic zygotes we observed had cumulus cells under the zona pellucida, which indicates its abnormal permeability; indeed, some of these eggs were fertilized by two or three spermatozoa. This suggests that androgenetic dispermic CHMs, known to account for approximately 15% of sporadic androgenetic CHMs,[2] may involve the same mechanism and occur also in conceptions from women with bi-allelic *MEI1* mutations.

The earliest defect that has been demonstrated in the oocytes from *Mei1*$^{-/-}$ and *Top6bl*$^{-/-}$ is the impaired double-strand breaks formation, which is essential for homologous chromosome synapsis and recombination. The absence of synapsis renders the meiotic silencing of unsynapsed chromatin regions, named MSUC, and affects subsequent meiotic processes depending on the silenced gene repertoire.[40–43] Consequently, *Mei1*$^{-/-}$ oocytes may have accumulated several defects including deficiency in cytoplasmic components in addition to chromosomes segregation errors. In humans, the MSUC can also be triggered by abnormal homologous chromosome synapsis in carriers of reciprocal translocations, which are well documented to be associated with infertility and recurrent miscarriages in male and female carriers.[44–46] With respect to HMs, two of the original reports about androgenetic monospermic CHMs found that 4%–6% of affected women had balanced chromosomal translocations, which is higher than the frequency of reciprocal translocation in the general population

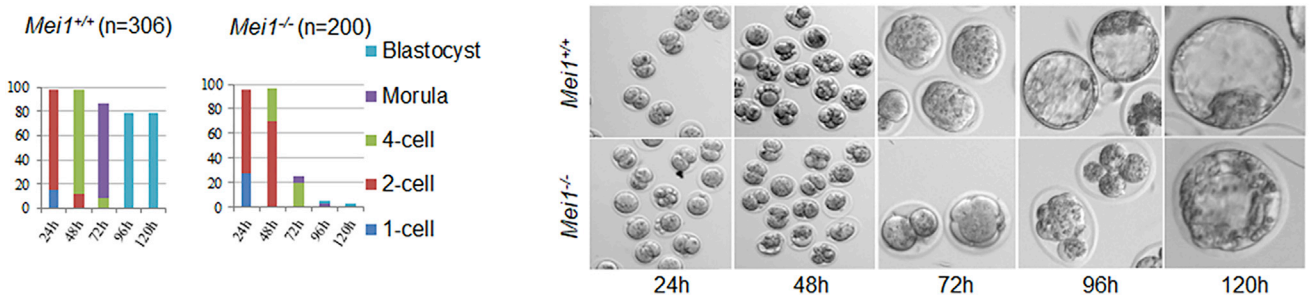

Figure 6. Preimplantation Development of *Mei1*$^{-/-}$ Oocytes in Culture
Zygotes were collected from wild-type or *Mei1*$^{-/-}$ females 20 hr after hCG injection and mating with wild-type males and cultured *in vitro*. Embryonic development was analyzed daily using phase contrast microscopy. The embryos that failed to develop by the next day were removed for further analysis. Embryos derived from *Mei1*$^{-/-}$ oocytes were arrested mainly at the 2- to 4-cell stage. A few reached the morula or blastocyst stages but appeared disorganized and none hatched.

(0.6%).[3,47] Miscarriages are a well-known risk factor for sporadic HMs[48] and sporadic HMs are more frequent in women with recurrent miscarriages than in women from the general population.[49,50] However, only weak associations have been reported between infertility problems, difficulties in conception, and irregular menstrual cycles and CHMs,[51,52] which may need to be revisited in the light of our findings. In *Mei1*-null oocytes, the spectrum of abnormalities ranged from oocytes with normal appearing chromosome complement (that would lead to euploid conceptions or aneuploid conceptions involving few chromosomes) to oocytes with few chromosomes (that would lead to severely aneuploid conceptions that may not survive implantation and lead to infertility) and empty oocytes (that would lead to androgenetic HMs), which support the commonalties between HM, miscarriages, and infertility observed in our affected women. In addition to the role of normal *Mei1* in double-strand breaks formation, in *C. elegans*, *mei1* has been shown to have a role in microtubule-severing activity similar to katanin;[53,54] consequently, its bi-allelic mutations may have prevented the disassembly of microtubules and the separation of the two sets of chromosomes at the spindle poles and favored their extrusion altogether into the PB. Investigating the possible occurrence of empty oocytes in null mice for *Top6bl* and *Rec114*, with no known roles in microtubule disassembly, will help clarifying which *Mei1* function is most likely at the origin of the extrusion of the oocyte chromosomes and spindles into the PB.

In conclusion, we unravel a mechanism, i.e., the extrusion of all the oocytes chromosomes with their spindles into the first PB, for the genesis of androgenetic zygotes in mammals and therefore a plausible mechanism for the genesis of AnCHMs in humans.

Accession Numbers

The patient accession numbers for *MEI1* variants are LOVD: 00181110 and 00181111, for *C11orf80* variants are LOVD: 00181112 and 00181113, and for *REC114* variants is LOVD: 00181114.

Supplemental Data

Supplemental Data include 11 figures, 5 tables, and 2 videos and can be found with this article online at https://doi.org/10.1016/j.ajhg.2018.10.007.

Acknowledgments

We thank Maria Galvez for her help in communicating with some individuals and coordinating the collection of samples from family members; Nawel Mechtouf and Yassemine Khawajkie for recruiting individuals and retrieving and analyzing some HM tissues; Xiao Yun Zhang for her help in the collection of human oocytes; Conceptions Reproductive Associates of Colorado for providing medical information; and Jyun-Yuan Huang, Pao-Lin Kuo, Farah Khan, and Surksha Agrawal for providing samples from individuals with recurrent miscarriages. We acknowledge the use of the McGill University and Génome Québec Innovation Centre for whole exome, Sanger, and targeted sequencing. We also acknowledge the use of Molecular Imaging Platform of the Research Institute of the McGill University Health Centre and thank Min Fu and Shibo Feng for their invaluable help. N.M.P.N. was supported by the RQR, McGill Faculty of Medicine, RI-MUHC, Desjardins Studentship in Child Heath Research, and the CRRD. This work was supported by the Canadian Institute of Health Research (MOP-130364) to R. Slim.

Declaration of Interests

The authors declare no competing interests.

Received: July 30, 2018
Accepted: October 3, 2018
Published: November 1, 2018

Web Resources

1000 Genomes, http://www.internationalgenome.org/
Combined Annotation Dependent Depletion (CADD), https://cadd.gs.washington.edu/
ExAC Browser, http://exac.broadinstitute.org/
LOVD, http://www.lovd.nl/3.0/home
MMRRC, http://www.csbio.unc.edu/MMRRC/index.py
MutationTaster, http://www.mutationtaster.org/
NCBI HomoloGene, http://www.ncbi.nlm.nih.gov/homologene

NHLBI Exome Sequencing Project (ESP) Exome Variant Server, http://evs.gs.washington.edu/EVS/
OMIM, http://www.omim.org/
Picard, http://broadinstitute.github.io/picard/
PolyPhen-2, http://genetics.bwh.harvard.edu/pph2/
SIFT, http://sift.bii.a-star.edu.sg/

References

1. Savage, P., Williams, J., Wong, S.L., Short, D., Casalboni, S., Catalano, K., and Seckl, M. (2010). The demographics of molar pregnancies in England and Wales from 2000-2009. J. Reprod. Med. *55*, 341–345.
2. Banet, N., DeScipio, C., Murphy, K.M., Beierl, K., Adams, E., Vang, R., and Ronnett, B.M. (2014). Characteristics of hydatidiform moles: analysis of a prospective series with p57 immunohistochemistry and molecular genotyping. Mod. Pathol. *27*, 238–254.
3. Kajii, T., and Ohama, K. (1977). Androgenetic origin of hydatidiform mole. Nature *268*, 633–634.
4. Golubovsky, M.D. (2003). Postzygotic diploidization of triploids as a source of unusual cases of mosaicism, chimerism and twinning. Hum. Reprod. *18*, 236–242.
5. Berkowitz, R.S., Im, S.S., Bernstein, M.R., and Goldstein, D.P. (1998). Gestational trophoblastic disease. Subsequent pregnancy outcome, including repeat molar pregnancy. J. Reprod. Med. *43*, 81–86.
6. Boufettal, H., Coullin, P., Mahdaoui, S., Noun, M., Hermas, S., and Samouh, N. (2011). [Complete hydatiforme mole in Morocco: epidemiological and clinical study]. J. Gynecol. Obstet. Biol. Reprod. (Paris) *40*, 419–429.
7. Horn, L.C., Kowalzik, J., Bilek, K., Richter, C.E., and Einenkel, J. (2006). Clinicopathologic characteristics and subsequent pregnancy outcome in 139 complete hydatidiform moles. Eur. J. Obstet. Gynecol. Reprod. Biol. *128*, 10–14.
8. Kim, J.H., Park, D.C., Bae, S.N., Namkoong, S.E., and Kim, S.J. (1998). Subsequent reproductive experience after treatment for gestational trophoblastic disease. Gynecol. Oncol. *71*, 108–112.
9. Kronfol, N.M., Iliya, F.A., and Hajj, S.N. (1969). Recurrent hydatidiform mole: a report of five cases with review of the literature. J. Med. Liban. *22*, 507–520.
10. Sebire, N.J., Fisher, R.A., Foskett, M., Rees, H., Seckl, M.J., and Newlands, E.S. (2003). Risk of recurrent hydatidiform mole and subsequent pregnancy outcome following complete or partial hydatidiform molar pregnancy. BJOG *110*, 22–26.
11. Murdoch, S., Djuric, U., Mazhar, B., Seoud, M., Khan, R., Kuick, R., Bagga, R., Kircheisen, R., Ao, A., Ratti, B., et al. (2006). Mutations in NALP7 cause recurrent hydatidiform moles and reproductive wastage in humans. Nat. Genet. *38*, 300–302.
12. Parry, D.A., Logan, C.V., Hayward, B.E., Shires, M., Landolsi, H., Diggle, C., Carr, I., Rittore, C., Touitou, I., Philibert, L., et al. (2011). Mutations causing familial biparental hydatidiform mole implicate c6orf221 as a possible regulator of genomic imprinting in the human oocyte. Am. J. Hum. Genet. *89*, 451–458.
13. Nguyen, N.M.P., Khawajkie, Y., Mechtouf, N., Rezaei, M., Breguet, M., Kurvinen, E., Jagadeesh, S., Solmaz, A.E., Aguinaga, M., Hemida, R., et al. (2018). The genetics of recurrent hydatidiform moles: new insights and lessons from a comprehensive analysis of 113 patients. Mod. Pathol. *31*, 1116–1130.
14. Eagles, N., Sebire, N.J., Short, D., Savage, P.M., Seckl, M.J., and Fisher, R.A. (2016). Risk of recurrent molar pregnancies following complete and partial hydatidiform moles. Hum. Reprod. *31*, 1379.
15. Libby, B.J., De La Fuente, R., O'Brien, M.J., Wigglesworth, K., Cobb, J., Inselman, A., Eaker, S., Handel, M.A., Eppig, J.J., and Schimenti, J.C. (2002). The mouse meiotic mutation mei1 disrupts chromosome synapsis with sexually dimorphic consequences for meiotic progression. Dev. Biol. *242*, 174–187.
16. Robert, T., Nore, A., Brun, C., Maffre, C., Crimi, B., Bourbon, H.M., and de Massy, B. (2016). The TopoVIB-Like protein family is required for meiotic DNA double-strand break formation. Science *351*, 943–949.
17. Kumar, R., Bourbon, H.M., and de Massy, B. (2010). Functional conservation of Mei4 for meiotic DNA double-strand break formation from yeasts to mice. Genes Dev. *24*, 1266–1280.
18. Reddy, R., Fahiminiya, S., El Zir, E., Mansour, A., Megarbane, A., Majewski, J., and Slim, R. (2014). Molecular genetics of the Usher syndrome in Lebanon: identification of 11 novel protein truncating mutations by whole exome sequencing. PLoS ONE *9*, e107326.
19. Li, H., and Durbin, R. (2009). Fast and accurate short read alignment with Burrows-Wheeler transform. Bioinformatics *25*, 1754–1760.
20. McKenna, A., Hanna, M., Banks, E., Sivachenko, A., Cibulskis, K., Kernytsky, A., Garimella, K., Altshuler, D., Gabriel, S., Daly, M., and DePristo, M.A. (2010). The Genome Analysis Toolkit: a MapReduce framework for analyzing next-generation DNA sequencing data. Genome Res. *20*, 1297–1303.
21. Li, H., Handsaker, B., Wysoker, A., Fennell, T., Ruan, J., Homer, N., Marth, G., Abecasis, G., Durbin, R.; and 1000 Genome Project Data Processing Subgroup (2009). The Sequence Alignment/Map format and SAMtools. Bioinformatics *25*, 2078–2079.
22. Wang, K., Li, M., and Hakonarson, H. (2010). ANNOVAR: functional annotation of genetic variants from high-throughput sequencing data. Nucleic Acids Res. *38*, e164.
23. Thorvaldsdóttir, H., Robinson, J.T., and Mesirov, J.P. (2013). Integrative Genomics Viewer (IGV): high-performance genomics data visualization and exploration. Brief. Bioinform. *14*, 178–192.
24. Taylor, D.M., Handyside, A.H., Ray, P.F., Dibb, N.J., Winston, R.M., and Ao, A. (2001). Quantitative measurement of transcript levels throughout human preimplantation development: analysis of hypoxanthine phosphoribosyl transferase. Mol. Hum. Reprod. *7*, 147–154.
25. Sahoo, T., Dzidic, N., Strecker, M.N., Commander, S., Travis, M.K., Doherty, C., Tyson, R.W., Mendoza, A.E., Stephenson, M., Dise, C.A., et al. (2017). Comprehensive genetic analysis of pregnancy loss by chromosomal microarrays: outcomes, benefits, and challenges. Genet. Med. *19*, 83–89.
26. Libby, B.J., Reinholdt, L.G., and Schimenti, J.C. (2003). Positional cloning and characterization of Mei1, a vertebrate-specific gene required for normal meiotic chromosome synapsis in mice. Proc. Natl. Acad. Sci. USA *100*, 15706–15711.
27. Xu, B., Noohi, S., Shin, J.S., Tan, S.L., and Taketo, T. (2014). Bidirectional communication with the cumulus cells is involved in the deficiency of XY oocytes in the components essential for proper second meiotic spindle assembly. Dev. Biol. *385*, 242–252.

28. Hu, M.W., Wang, Z.B., Jiang, Z.Z., Qi, S.T., Huang, L., Liang, Q.X., Schatten, H., and Sun, Q.Y. (2014). Scaffold subunit Aalpha of PP2A is essential for female meiosis and fertility in mice. Biol. Reprod. *91*, 19.
29. Cartegni, L., Chew, S.L., and Krainer, A.R. (2002). Listening to silence and understanding nonsense: exonic mutations that affect splicing. Nat. Rev. Genet. *3*, 285–298.
30. Holbrook, J.A., Neu-Yilik, G., Hentze, M.W., and Kulozik, A.E. (2004). Nonsense-mediated decay approaches the clinic. Nat. Genet. *36*, 801–808.
31. Hiraoka, Y., Ding, D.Q., Yamamoto, A., Tsutsumi, C., and Chikashige, Y. (2000). Characterization of fission yeast meiotic mutants based on live observation of meiotic prophase nuclear movement. Chromosoma *109*, 103–109.
32. Maleki, S., Neale, M.J., Arora, C., Henderson, K.A., and Keeney, S. (2007). Interactions between Mei4, Rec114, and other proteins required for meiotic DNA double-strand break formation in *Saccharomyces cerevisiae*. Chromosoma *116*, 471–486.
33. Grelon, M., Gendrot, G., Vezon, D., and Pelletier, G. (2003). The *Arabidopsis* MEI1 gene encodes a protein with five BRCT domains that is involved in meiosis-specific DNA repair events independent of SPO11-induced DSBs. Plant J. *35*, 465–475.
34. Mains, P.E., Kemphues, K.J., Sprunger, S.A., Sulston, I.A., and Wood, W.B. (1990). Mutations affecting the meiotic and mitotic divisions of the early *Caenorhabditis elegans* embryo. Genetics *126*, 593–605.
35. Ben Khelifa, M., Ghieh, F., Boudjenah, R., Hue, C., Fauvert, D., Dard, R., Garchon, H.J., and Vialard, F. (2018). A MEI1 homozygous missense mutation associated with meiotic arrest in a consanguineous family. Hum. Reprod. *33*, 1034–1037.
36. Mahadevan, S., Wen, S., Balasa, A., Fruhman, G., Mateus, J., Wagner, A., Al-Hussaini, T., and Van den Veyver, I.B. (2013). No evidence for mutations in NLRP7 and KHDC3L in women with androgenetic hydatidiform moles. Prenat. Diagn. *33*, 1242–1247.
37. Miao, Y., Ma, S., Liu, X., Miao, D., Chang, Z., Luo, M., and Tan, J. (2004). Fate of the first polar bodies in mouse oocytes. Mol. Reprod. Dev. *69*, 66–76.
38. Liu, H., Kim, J.M., and Aoki, F. (2004). Regulation of histone H3 lysine 9 methylation in oocytes and early pre-implantation embryos. Development *131*, 2269–2280.
39. Clark-Maguire, S., and Mains, P.E. (1994). Localization of the mei-1 gene product of *Caenorhaditis elegans*, a meiotic-specific spindle component. J. Cell Biol. *126*, 199–209.
40. Baarends, W.M., Wassenaar, E., van der Laan, R., Hoogerbrugge, J., Sleddens-Linkels, E., Hoeijmakers, J.H., de Boer, P., and Grootegoed, J.A. (2005). Silencing of unpaired chromatin and histone H2A ubiquitination in mammalian meiosis. Mol. Cell. Biol. *25*, 1041–1053.
41. Turner, J.M., Mahadevaiah, S.K., Fernandez-Capetillo, O., Nussenzweig, A., Xu, X., Deng, C.X., and Burgoyne, P.S. (2005). Silencing of unsynapsed meiotic chromosomes in the mouse. Nat. Genet. *37*, 41–47.
42. Carofiglio, F., Inagaki, A., de Vries, S., Wassenaar, E., Schoenmakers, S., Vermeulen, C., van Cappellen, W.A., Sleddens-Linkels, E., Grootegoed, J.A., Te Riele, H.P., et al. (2013). SPO11-independent DNA repair foci and their role in meiotic silencing. PLoS Genet. *9*, e1003538.
43. Schimenti, J. (2005). Synapsis or silence. Nat. Genet. *37*, 11–13.
44. Ferguson, K.A., Chow, V., and Ma, S. (2008). Silencing of unpaired meiotic chromosomes and altered recombination patterns in an azoospermic carrier of a t(8;13) reciprocal translocation. Hum. Reprod. *23*, 988–995.
45. Pujol, A., Durban, M., Benet, J., Boiso, I., Calafell, J.M., Egozcue, J., and Navarro, J. (2003). Multiple aneuploidies in the oocytes of balanced translocation carriers: a preimplantation genetic diagnosis study using first polar body. Reproduction *126*, 701–711.
46. Anton, E., Vidal, F., and Blanco, J. (2008). Reciprocal translocations: tracing their meiotic behavior. Genet. Med. *10*, 730–738.
47. Lawler, S.D., Fisher, R.A., Pickthall, V.J., Povey, S., and Evans, M.W. (1982). Genetic studies on hydatidiform moles. I. The origin of partial moles. Cancer Genet. Cytogenet. *5*, 309–320.
48. Altieri, A., Franceschi, S., Ferlay, J., Smith, J., and La Vecchia, C. (2003). Epidemiology and aetiology of gestational trophoblastic diseases. Lancet Oncol. *4*, 670–678.
49. Coulam, C.B. (1991). Epidemiology of recurrent spontaneous abortion. Am. J. Reprod. Immunol. *26*, 23–27.
50. Acaia, B., Parazzini, F., La Vecchia, C., Ricciardiello, O., Fedele, L., and Battista Candiani, G. (1988). Increased frequency of complete hydatidiform mole in women with repeated abortion. Gynecol. Oncol. *31*, 310–314.
51. La Vecchia, C., Franceschi, S., Parazzini, F., Fasoli, M., Decarli, A., Gallus, G., and Tognoni, G. (1985). Risk factors for gestational trophoblastic disease in Italy. Am. J. Epidemiol. *121*, 457–464.
52. Berkowitz, R.S., Bernstein, M.R., Harlow, B.L., Rice, L.W., Lage, J.M., Goldstein, D.P., and Cramer, D.W. (1995). Case-control study of risk factors for partial molar pregnancy. Am. J. Obstet. Gynecol. *173*, 788–794.
53. Srayko, M., Buster, D.W., Bazirgan, O.A., McNally, F.J., and Mains, P.E. (2000). MEI-1/MEI-2 katanin-like microtubule severing activity is required for *Caenorhabditis elegans* meiosis. Genes Dev. *14*, 1072–1084.
54. McNally, K., Audhya, A., Oegema, K., and McNally, F.J. (2006). Katanin controls mitotic and meiotic spindle length. J. Cell Biol. *175*, 881–891.